

Transcriptional memory-like imprints and enhanced functional activity in  $\gamma\delta$  T cells  
following resolution of malaria infection

Rasika Kumarasingha\*,<sup>1,2</sup> Lisa J. Ioannidis\*,<sup>1,2</sup> Waruni Abeysekera,<sup>1,2</sup> Stephanie Studniberg,<sup>1,2</sup> Dinidu Wijesurendra,<sup>1,2</sup> Ramin Mazhari,<sup>1,2</sup> Daniel P. Poole,<sup>3</sup> Ivo Mueller,<sup>1,2</sup> Louis Schofield,<sup>1,4,5</sup> Diana S. Hansen<sup>1,2</sup> and Emily M. Eriksson<sup>1,2#</sup>

\* Equal contribution

1. Walter and Eliza Hall Institute of Medical Research, VIC 3052, Australia
2. The University of Melbourne, Department of Medical Biology, VIC 3052, Australia
3. Drug Discovery Biology, Monash Institute of Pharmaceutical Sciences, Monash University VIC 3052, Australia
4. School of Veterinary and Biomedical Sciences, James Cook University, QLD 4811, Australia.
5. Australian Institute of Tropical Health and Medicine, James Cook University, QLD 4811, Australia

#Corresponding Author:

Emily M. Eriksson

The Walter and Eliza Hall Institute of Medical Research

1G Royal Parade, VIC 3052, Australia

Tel: +61 3 93452870, Fax: +61 3 93470852, email: [eriksson@wehi.edu.au](mailto:eriksson@wehi.edu.au)

## Abstract

$\gamma\delta$  T cells play an essential role in the immune response to malaria infection. However, long-lasting effects of malaria infection on the  $\gamma\delta$  T cell population still remain inadequately understood. This study investigated transcriptional changes and memory-like functional capacity of malaria pre-exposed  $\gamma\delta$  T cells using a *Plasmodium chabaudi* infection model. We show that multiple genes associated with effector function (chemokines, cytokines and cytotoxicity) and antigen-presentation were upregulated in *P. chabaudi*-exposed  $\gamma\delta$  T cells compared to  $\gamma\delta$  T cells from naïve mice. This transcriptional profile was positively correlated with profiles observed in conventional memory CD8<sup>+</sup> T cells and was accompanied by enhanced reactivation upon secondary encounter with *Plasmodium*-infected red blood cells *in vitro*. Collectively our data demonstrate that *Plasmodium* exposure result in “memory-like imprints” in the  $\gamma\delta$  T cell population and also promotes  $\gamma\delta$  T cells that can support antigen-presentation during subsequent infections.

## Introduction

$\gamma\delta$  T cells are unconventional T cells that display characteristic features of both innate and adaptive immunity. Their capacity to respond rapidly to non-peptide antigens in an MHC-independent manner places them as part of the innate first line of defense against numerous pathogens. Additionally, emerging evidence supports the concept that  $\gamma\delta$  T cells also display memory T cell-like abilities. This includes prolonged recall responses upon reinfection in various disease and vaccine models, which contribute to protective immunity<sup>1-6</sup>. Recent studies have now started to delineate a more in-depth understanding of these adaptive-like  $\gamma\delta$  T cells. For example, it has been described that the TCR of tissue-resident  $\gamma\delta$  T cells has an intrinsic ability to distinguish between distinct antigen-stimulus and in this way promote either clonal or non-clonal responses<sup>7</sup> whereas adaptive-like  $\gamma\delta$  T cells found in peripheral human blood are suggested to be restricted to specific subsets of the  $\gamma\delta$  T cell population<sup>8</sup>.

*Plasmodium* infection, which is responsible for the induction of malaria in humans, elicits a multifaceted response activating a wide range of immune cells, including  $\gamma\delta$  T cells. Extensive evidence shows that  $\gamma\delta$  T cells are part of the immediate innate response during human malaria infection where they are found to be cytotoxically active and produce cytokines associated with both protective immunity and symptomatic episodes<sup>9-15</sup>. The underlying mechanisms by which  $\gamma\delta$  T cells either contribute to beneficial outcomes in the host or mediate pathogenesis remain to be fully elucidated. However, studies using field samples indicate that repeated exposure to the parasite promotes  $\gamma\delta$  T cells that are associated with the development of clinical symptoms<sup>13-15</sup> in an infected individual. In contrast,  $\gamma\delta$  T cells have been proposed to

be part of the IFN $\gamma$ -producing memory pool found upon re-exposure in experimentally controlled-malaria infected individuals<sup>16</sup>.

In addition to human infections,  $\gamma\delta$  T cells are also highly involved in the immune response to murine malaria. In mice, they are a major source of cytokines and contribute to parasite clearance<sup>17-22</sup> and are essential for protective immunity following vaccination<sup>23</sup>. This makes murine malaria infection models a useful platform to explore fundamental immunological questions related to *Plasmodium* infection and also enables the investigation of immune populations within various tissues not readily available from infected individuals. *P. chabaudi* infection in C57BL/6 mice is a self-resolving infection, and this infection model has been used to successfully elucidate various aspects of  $\gamma\delta$  T cell biology.  $\gamma\delta$  T cells proliferate extensively in response to *P. chabaudi* infection and mice lacking  $\gamma\delta$  T cells experience exacerbated parasitemia<sup>21, 24-26</sup>. More recently,  $\gamma\delta$  T cells from chronically infected mice were described to produce inflammatory chemokines such as CCL3 and CCL5 and also importantly m-CSF, which was vital to the control of recrudescence<sup>19</sup> suggesting that “antigen-experienced”  $\gamma\delta$  T cells play a role in the suppression of parasitemia in chronic infection. Although these studies further emphasize that  $\gamma\delta$  T cells are readily activated during acute *Plasmodium* infection, the lasting effect that *Plasmodium* exposure has on these cells and how this shapes the  $\gamma\delta$  T cell population is still inadequately understood. Consequently, we used the *P. chabaudi* murine malaria infection model to investigate transcriptional profiles of  $\gamma\delta$  T cells from naïve and malaria-exposed mice, 12 weeks after completion of anti-malarial drug treatment. Our findings revealed that antigen-experienced  $\gamma\delta$  T cells display a transcriptional profile that shares features with that of conventional memory CD8<sup>+</sup> T cells and have

enhanced functional capacity. Thus, our data support the notion that  $\gamma\delta$  T cells differentiate and acquire a memory-like phenotype after infection. These observations advance our basic understanding of unconventional T cell biology in malaria but may also give insight into how responses to vaccines or other pathogens can be affected by malaria pre-exposure.

## Results

### **Increased frequencies of multifunctional $\gamma\delta$ T cells in drug-cured *P. chabaudi*-exposed mice**

The hallmark of memory T cells is increased functional capacity upon secondary encounter with specific antigen, which commonly includes IFN $\gamma$  production and cytotoxic activity. To establish whether similar responses were generated in  $\gamma\delta$  T cells following *Plasmodium* infection, we compared responses of naïve and pre-exposed  $\gamma\delta$  T cells upon antigen re-encounter. Since spleen and liver are central to the immune response to *P. chabaudi* infection<sup>27, 28</sup> and are organs that have previously been shown to contain tissue resident innate memory cells<sup>29, 30</sup>, we assessed  $\gamma\delta$  T cell responses in both of these organs. To that end, C57BL/6 mice were infected with *P. chabaudi* and drug-cured on day 14 post-infection (p.i.) to clear parasitemia completely. Twelve weeks after completion of drug-treatment spleens and livers were harvested (Figure 1A). Splenocytes and liver lymphocytes were subsequently isolated and stimulated *in vitro* with *P. chabaudi*-infected red blood cells (iRBC) or uninfected RBC (uRBC) as background controls. Cells from naïve mice were included to measure baseline responses. After a 24 h incubation, CD107a surface expression (as a measure of cytotoxic activity) and IFN $\gamma$  production were assessed by flow cytometry (Figure 1B). We found that a significantly higher frequency of  $\gamma\delta$  T cells that were

both CD107a<sup>+</sup> and produced IFN $\gamma$  were present in the spleens of previously infected mice compared to naïve mice (Figure 1C, P< 0.0001). No significant differences were observed with  $\gamma\delta$  T cells that produced only IFN $\gamma$  or were CD107a<sup>+</sup>. Similarly, no significant differences in functionality were detected in the liver-derived  $\gamma\delta$  T cells from pre-exposed *P. chabaudi*-infected mice and naïve mice (Figure 1D). This showed that *P. chabaudi* infection resulted in the induction of multi-functional memory-like  $\gamma\delta$  T cells.

### **Responding $\gamma\delta$ T cells express an effector memory-like phenotype**

Previous studies indicate that the  $\gamma\delta$  T cells that provide effector functions during acute malaria infection express surface markers that resemble conventional  $\alpha\beta$  T effector memory cells<sup>16,19</sup>. To assess the phenotype of the responding  $\gamma\delta$  T cells of previously exposed mice after full resolution of infection, we stimulated spleen-derived  $\gamma\delta$  T cells from drug-treated mice or naïve mice *in vitro* and stained the cells for the surface markers CD62L and CD44. This enabled the  $\gamma\delta$  T cells to be subdivided into CD62L<sup>+</sup>CD44<sup>-</sup> naïve cells, CD62L<sup>+</sup>CD44<sup>+</sup> central memory cells (CM) and CD62L<sup>-</sup>CD44<sup>+</sup> effector memory cells (EM; Figure 2A). The frequency of IFN $\gamma$ <sup>+</sup>CD107a<sup>+</sup> double positive  $\gamma\delta$  T cells in each subset was assessed in both groups of mice. Representative flow cytometry plots of these responses are presented in Figure 2B. Upon stimulation with iRBC, responding  $\gamma\delta$  T cells were found to predominantly express an EM phenotype and frequencies of IFN $\gamma$ <sup>+</sup>CD107a<sup>+</sup> EM  $\gamma\delta$  T cells were significantly higher in previously *P. chabaudi*-infected mice compared to naïve control mice (P< 0.0001; Figure 2C). This demonstrated that  $\gamma\delta$  T memory-like responses were specifically confined within the EM subset. Furthermore, the increase

in frequency of responding cells did not reflect an overall increase of EM  $\gamma\delta$  T cells in the pre-exposed mice as assessment of the  $\gamma\delta$  T cell composition showed no differences in frequencies (Figure 2D) or cell numbers (Figure 2E) of naïve, CM or EM  $\gamma\delta$  T cells between *P. chabaudi* exposed mice and uninfected controls.

### **Transcriptional profile changes in EM $\gamma\delta$ T cells from drug-treated *P. chabaudi* exposed mice compared to EM $\gamma\delta$ T cells from naïve mice**

We have shown that  $\gamma\delta$  T cells expressing an EM-phenotype are re-activated upon re-encounter with *P. chabaudi* iRBC in previously infected mice (Figure 2). As the frequency and number of EM  $\gamma\delta$  T cells in the spleens were not different between the naïve control group and the pre-exposed mice, this indicated that this memory-like enhanced responsiveness was due to intrinsic changes of the cells. To investigate this, EM  $\gamma\delta$  T cells were FACS-sorted from mice 12 weeks after they had been drug treated to clear *P. chabaudi* infection (n=5) and from naïve mice (n=5; Figure 3) and RNA-sequencing was used to examine transcriptional profiles. A total of 207 differentially expressed (DE) genes in *P. chabaudi* pre-exposed EM  $\gamma\delta$  T cells compared to EM  $\gamma\delta$  T cells from naïve mice were observed relative to a fold change threshold of 1.5 (Supplemental Table 1). Expression levels and log-fold changes were plotted in a Mean-Difference (MD) plot (Figure 3A) of which 96 genes were significantly upregulated (indicated in red) and 111 genes were significantly down regulated (indicated in blue). The upregulated genes included MHC class II-related genes (H2-Dmb2 and H2-A) and also IFN $\gamma$  and NKg7, which corresponded to the observed functional phenotype of enhanced IFN $\gamma$  production and cytotoxicity in the

pre-exposed EM  $\gamma\delta$  T cells (Figure 2). The chemokine genes (CCL3, CCL4 and CCL5) were also upregulated in these memory-like  $\gamma\delta$  T cells, which is similar to what had previously been reported to be upregulated in  $\gamma\delta$  T cells during an active infection (Mamedov 2018). Cytokine receptor genes (Il1r and Il23r), scavenger-receptor gene (Cd163l1) and transcription factor gene (Sox13) were among the down regulated genes. The top 75 DE genes are summarized in a heatmap presenting up- and down regulated genes in each mouse (Figure 3B). Collectively, this shows that malaria-infection causes significant transcriptional changes in the EM  $\gamma\delta$  T cell population, which is still observed in absence of an active infection.

### **Genes involved in antigen presentation and processing are upregulated in pre-exposed EM $\gamma\delta$ T cells**

To understand the biological processes affected by previous exposure to malaria in the EM  $\gamma\delta$  T cell population, gene ontology (GO) pathway analysis was performed. Among the twenty most highly enriched GO terms in the upregulated biological processes, 7 were associated with antigen-processing and presentation. In addition, genes were enriched for processes involving positive regulation of acute inflammatory responses and response to IFN $\gamma$  (Supplemental Figure 1A). Barcode plots and bar plots illustrating the enrichment of all genes in selected pathways showed that antigen-processing and presentation pathway included upregulation of MHC class II-related genes (H2-Aa, H2-Dmb2, H2-Ab1, H2-Eb1, H2-Dmb1), genes that support antigen-processing and presentation (Clec4a2, Flt3, Cd74, Ifng) and genes for FC receptor expression (Fcrgr2b, Fcer1g; Figure 4A). There were also



enrichment of genes that suggested an increased responsiveness to IFN $\gamma$  stimulation as shown by upregulation of chemokine and cytokine genes (Ccl3, Ccl4, Ccl5, Ifng, Xcl1), interferon induced transmembrane protein genes (Ifitm2, Ifitm3) and MHC class II-related genes (H2-Aa, H2-Ab1, H2-Eb1), but down regulation of IL23r (Figure 4B). In addition, gene enrichment analysis suggested that pre-exposed EM  $\gamma\delta$  T cells have the potential to contribute to a sustained inflammatory response as shown by upregulation of Fcer1a, Alox5bp, Ptgs2, Fcer1g and Ccl5 combined with down regulation of Adam8 (Figure 4C).

Some of the most significantly down regulated biological processes included cell-substrate adhesion and cellular response to stimulus (Supplemental Figure 1B). Considering that responsiveness to IFN $\gamma$  stimulation was increased (Supplemental Figure 1A), decrease in the biological process of cellular response to stimulus suggests that the pre-exposed EM  $\gamma\delta$  T cell population is modulated to only respond to specific conditions such as presence of IFN $\gamma$ . Barcode plots and bar plots illustrating the enrichment of all genes in these down regulated pathways showed that a total of 85 DE genes were represented in the cellular response to stimulus (Figure 5A). The 3 most down regulated genes in this pathway were Itgb4, Plxnd1 and Tspan2, which are all associated with signal transduction and cell-cell signaling. The most upregulated gene in this pathway was Fcer1a, which has been associated with an immune suppressive role in APCs<sup>31</sup>. The enrichment of all genes in the cell-substrate adhesion pathway included down regulated integrin genes (Itgb4, Itga5, Itgb5), protein kinases (Trmp7, Slk) and genes associated with cell recruitment, adhesion and

migration (Adam8, Jag1, Lamc1, L1cam) whereas Epdr and Smoc2 genes were upregulated (Figure 5B).

**Differentially expressed genes in pre-exposed EM  $\gamma\delta$  T cells are positively correlated with differentially expressed genes in resting memory CD8<sup>+</sup> T cells.**

A previous study demonstrated that conventional CD8<sup>+</sup> memory T cells have distinct transcriptional profiles that significantly differ from those of their naïve counterparts<sup>32</sup>. To examine whether the transcriptional profile observed in the pre-exposed  $\gamma\delta$  T cells resembled that of conventional memory T cells, we compared our DE expression data (Supplemental Table 1) with a previously described signature defining resting CD8<sup>+</sup> memory T cells<sup>32</sup> (Russ et al. Supplemental Table 2). A total of 43 DE genes were represented in both gene sets, of which 32 were upregulated and 11 were down regulated DE genes (Figure 6A). These overlapping genes presented in a heatmap (Figure 6B) included genes that were associated with hallmark functions of conventional memory T cells such as cytokine/chemokine production and cytotoxicity (Ccl4, Ccl5, Ccl3, Ifng, Nkg7). Genes involved in antigen presentation and processing (Clec4a2, Fcgr2b, H2-Aa, H2-Dmb2, H2-Ab1, H2-Eb1, Cd74, H2-Dmb1, Fcer1g), which was a prominent transcriptional signature of the memory-like EM  $\gamma\delta$  T cell DE gene set, also overlapped with the DE genes from CD8<sup>+</sup> memory T cells. Furthermore, enrichment analysis showed that both up and down regulated DE genes in the EM  $\gamma\delta$  T cell gene set positively correlated with the DE genes in the CD8<sup>+</sup> memory T cell gene set (P= 0.008; Figure 6C). Altogether, this supports the novel concept that *Plasmodium* exposure induces EM  $\gamma\delta$  T cells with a transcriptional profile resembling conventional memory T cells.

## Discussion

Immunological memory is considered a definitive feature of adaptive immunity, allowing clonal selection of antigen-specific T and B lymphocytes where differentiation to memory cells is the basis for enhanced secondary responses to subsequent challenge. In contrast, innate immunity was long considered to lack such memory features and instead rely on a repertoire of invariant receptors. However, recent studies demonstrate that a number of cells of the innate immune system have the capacity to establish immunological memory. Emerging functional evidence suggest that this includes  $\gamma\delta$  T cells in specific disease models<sup>2,33</sup>. However, whether exposure to antigen induces transcriptional profiles in EM  $\gamma\delta$  T cells associated with enhanced effector function have remained elusive. In this study we used a malaria infection model to understand whether “memory-like imprints” were detectable in  $\gamma\delta$  T cells after the infection was cleared and whether this was associated with memory-like  $\gamma\delta$  T cell responses. We found that the transcriptional profile in pre-exposed EM  $\gamma\delta$  T cells was significantly different from EM  $\gamma\delta$  T cells from naïve mice and that differentially expressed genes in the pre-exposed EM  $\gamma\delta$  T cells were positively correlated with previously reported differentially expressed genes in resting CD8<sup>+</sup> memory T cells. This showed that although  $\gamma\delta$  T cell populations in both naïve mice and previously *P. chabaudi*-infected mice were classified as “memory” populations based on traditional surface markers, only pre-exposed  $\gamma\delta$  T cells were observed to resemble that of conventional T cell memory.

Consistent with their memory-like transcriptional profile, we also found that pre-exposure to antigen resulted in enhanced functional capacity of responding  $\gamma\delta$  T cells

upon encounter with cognate antigen. It has been suggested that as  $\gamma\delta$  T cells emerge from the thymus, they have already acquired a functional imprint, which limits their plasticity in the periphery<sup>34-36</sup>. Furthermore, functionally distinct  $\gamma\delta$  T cells seem to have specific tissue distribution where spleen-derived  $\gamma\delta$  T cells are predominately prone to producing IFN $\gamma$ <sup>34</sup>. We found that pre-exposed  $\gamma\delta$  T cells were multifunctional as they produced both IFN $\gamma$  and were cytotoxically active. However, the EM  $\gamma\delta$  T cell population previously-exposed to malaria displayed significant reductions in the expression of genes associated with IL-17 responses, suggesting limitation to their functional plasticity after *Plasmodium* infection. Apart from low gene expression of IL-17a, this included significantly lower expression levels of *Sox13* and *Il1r1* genes. Sox13 is a lineage specific  $\gamma\delta$  T cell transcription factor<sup>37</sup>, which promotes IL-17 producing  $\gamma\delta$  T cells<sup>38</sup> and IL-1 has recently been indicated to play an important role in supporting IL-17 production by antigen-specific T cells *in vivo*. Cells from *Il1r1*-deficient mice had dramatically reduced IL-17 production compared to cells from wild-type mice<sup>39</sup>. Furthermore IL-17 producing  $\gamma\delta$  T cells have been shown to rapidly respond to IL-23, which induces and supports IL-17 production<sup>40-42</sup>. Interestingly following *Plasmodium* exposure, EM  $\gamma\delta$  T cells have down regulated their *Il-23r* gene expression suggesting that they are less responsive to endogenous IL-23. This indicates that the functionally intrinsic characteristics of EM  $\gamma\delta$  T cells is altered with infection and is maintained in absence of parasites.

We showed here that the  $\gamma\delta$  T cell population in the spleen not only acquires memory-like characteristics, but also potentially fill an additional role as APCs. Although antigen-presentation and processing by  $\gamma\delta$  T cells has previous been described, this

characteristic remains relatively unexplored. This function is seemingly acquired upon TCR activation and human V $\delta$ 2 T cells activated with isopentenyl pyrophosphate induced high levels of APC-related molecules, which resulted in a functional capacity to present antigens to  $\alpha\beta$  T cells<sup>43</sup>. In *P. falciparum*-infected individuals there is an increase of V $\gamma$ 9V $\delta$ 2 T cells that express APC-related surface markers and this expression was induced by iRBCs<sup>44</sup>. These cells were also able to elicit  $\alpha\beta$  T cell responses *in vitro* suggesting that  $\gamma\delta$  T cells may simply supplement existing APC populations. However, spleen-derived  $\gamma\delta$  T cells reside in an organ that plays a central role in the capacity to control and clear parasites and are in a location that allows them to encounter and remove blood-borne antigens and also initiate innate and adaptive immune responses. It is possible that following an initial malaria infection once an adaptive memory has been established, exposed  $\gamma\delta$  T cells promote specific adaptive T cell functions. In support of this proposition, intestinal  $\gamma\delta$  T cells have been found to have APC function and elicit distinct CD4<sup>+</sup> T cell responses compared to responses induced by typical professional APCs<sup>45</sup>. A comprehensive understanding of the APC-capacities of tissue-resident  $\gamma\delta$  T cells and the specific functions that they provide for subsequent *Plasmodium* infections remains to be determined.

The work presented here demonstrates that blood-stage *Plasmodium* infection has a profound effect on the splenic  $\gamma\delta$  T cell population, modifying its response capacity and gene expression profile. While our observations here support the existence of traditional memory cells with augmented secondary responses upon antigen re-encounter, it also appears that this functional capacity may not necessarily be the only role for these cells. Our findings here suggest a model by which antigen-experienced

$\gamma\delta$  T cells undergo transcriptional changes that allows them to fulfil a novel role as antigen-presenting cells in subsequent infections. These findings have important implications for our understanding of the role of  $\gamma\delta$  T cells in host immunity and gives insight into potential therapeutic modulations that can be achieved.

## **Material and Methods**

### **Mice and Mouse infection**

Female C57BL/6 mice aged 6-8 weeks were infected with  $5 \times 10^4$  *Plasmodium chabaudi* iRBC intravenously. All mice were drug-treated on day 14 p.i. with an intraperitoneal injection of chloroquine (CQ; 10mg/kg) and pyrimethamine (10mg/kg) followed by CQ (0.6 mg/ml) and pyrimethamine (70  $\mu$ g/ml) containing water for 5 days. Spleens and livers were removed 12 weeks after completion of drug treatment. The experimental design is summarized in Figure 1A. Organs from drug- treated naïve mice were used as controls. All procedures involving mice were approved by the Walter and Eliza Hall Institute animal ethics committee (2015.020).

### ***In vitro* cell stimulation**

Single cell suspensions from spleen or liver were prepared as previously described<sup>46</sup>. Wholeblood from *P. chabaudi*-infected donors were obtained during the dark cycle to obtain mature parasites<sup>47</sup>. The blood was washed in RPMI and 0.5-1 ml of blood in medium was overlaid onto 12.17 ml of a 74% percoll gradient as described in<sup>48</sup> and centrifuged at 5000 g for 20 min at room temperature. IRBCs were collected from the interface and washed with culture medium. Isolated iRBCs were co-incubated with splenocytes and liver lymphocytes at a ratio of 1:1 for 24 h. Brefeldin A (Sigma, St.

Louis, MO) and GolgiStop (BD Biosciences, San Jose, CA) were added for the final 8 h of incubation.

### **Flow Cytometry and FACS sorting**

A total of  $1 \times 10^6$  splenocytes or liver lymphocytes were surface stained with Brilliant Violet (BV) 421-conjugated anti-CD107a (clone 1D4B, BioLegend, San Diego, CA) during the 24 h stimulation. Further surface staining following stimulation was performed with antibody mixtures in FACS buffer (phosphate buffer saline containing 0.5% bovine serum albumin (BSA) and 2mM ethylenediaminetetraacetic acid (EDTA) on ice for 30 min. Antibodies used included: Fluorescein isothiocyanate (FITC)-conjugated anti-CD3 (clone 145-2C11), PerCP Cy5.5-conjugated anti- $\gamma\delta$ TCR (clone GL3), allophycocyanin (APC)-conjugated anti-CD27 (clone LG.3A10), (all from BioLegend), Alexa700-conjugated anti-CD44 (clone IM7) and Brilliant Violet (BV) 605-conjugated anti-CD62L (clone MEL-14, BD Biosciences, San Jose, CA). Aqua live/dead amine reactive dye (Life Technologies, Carlsbad, CA) was used for dead cell exclusion. Intracellular staining was performed after 2% paraformaldehyde fixation and permeabilization with Perm 2 buffer (BD Biosciences) using BV711-conjugated anti-IFN $\gamma$  (clone XMG1.2, BioLegend). Samples were analyzed on a customized four-laser Fortessa flow cytometer (BD Biosciences). Data analysis was performed using FlowJo 9.9.6 software (TreeStar, Ashland, OR) and Boolean gating. For FACS sorting, splenocytes were surface stained with CD3,  $\gamma\delta$ TCR, CD62L and CD44 as above to identify and collect  $\gamma\delta$  T cells with a phenotype associated with T effector memory (EM, CD62L<sup>-</sup> CD44<sup>+</sup>).

### **Library preparation and transcriptome sequencing**

EM  $\gamma\delta$  T cells from 5 naïve control mice and 5 mice that had been previously infected with *P. chabaudi* and then drug-treated to clear the infections were FACS sorted. Total RNA was isolated from sorted cells using the Isolate II RNA mini kit (Bioline, London, UK) according to manufacturer's instructions. RNA was quantified using the Agilent TapeStation 2200 system (Santa Clara, CA). An input of 1 ng of total RNA were prepared and indexed separately for sequencing using the Clontech SMART ultra-low RNA input Prep Kit (Illumina, San Diego, CA) as per manufacturer's instruction. The indexed libraries were pooled and diluted to 1.5pM for paired end sequencing (2x 76 cycles) on a NextSeq 500 instrument using the v2 150 cycle High Output kit (Illumina) as per manufacturer's instructions. The base calling and quality scoring were determined using Real-Time Analysis on board software v2.4.6, while the FASTQ file generation and de-multiplexing utilized bcl2fastq conversion software v2.15.0.4. Paired-end 75bp. Between 16 and 56 million read pairs were generated for each sample and reads were aligned to the *Mus musculus* genome (mm10) using the Subread aligner<sup>49</sup>. The number of read pairs overlapping each mouse Entrez gene was summarized using featureCount<sup>50</sup> and Subread's built-in NCBI gene annotation. Genes were filtered using filterByExpr function in edgeR<sup>51</sup> software package. Genes without current annotation and Immunoglobulin genes were also filtered. Differential expression (DE) analysis was undertaken using the edgeR and limma<sup>52</sup> software packages. Library sizes were normalized using the trimmed mean of M-values (TMM) method<sup>53</sup>. Log2 fold-changes were computed using voom<sup>54</sup>. Differential expression was assessed relative to a fold change threshold of 1.5 using the TREAT<sup>55</sup> function, a robust empirical Bayes procedure<sup>56</sup> implemented in the limma package. The false discovery rate (FDR) was controlled below 0.05 using the method of Benjamini and Hochberg<sup>57</sup>. Over-representation of Gene Ontology (GO) terms for



the differentially expressed genes was identified using the goana function in limma package. Barcode plots illustrating the enrichment of interested pathway genes were drawn using the barcode plot function in limma package<sup>58</sup>.

### **Statistical Analysis**

Statistical analyses were performed using Prism 8.0 (GraphPad software, San Diego, CA) Flow cytometry data was analyzed using the Student's t-test. Statistical significance was considered  $P \leq 0.05$

### **Acknowledgements**

We wish to thank Liana Mackiewicz and Carolina Alvarado at WEHI for technical assistance.

**Competing interests:** No competing interests exist.

**Author contribution:** RK and LJI performed experiments and critically reviewed the manuscript, WA and DPP analysed data and critically reviewed the manuscript, DW, RM and SS analysed data, IM, DSH and LS provided conceptual input into the study design and critically reviewed the manuscript, EME conceived and performed experiments, analysed data and prepared the manuscript.

**Funding:** This work was supported by NHMRC grant APP106722 (EE). This work was made possible through Victorian State Government Operational Infrastructure Support and Australian Government NHMRC IRIISS. I.M. is supported by an

NHMRC Senior Research Fellowship (#1043345). The funders had no role in study design, data collection and analysis, decision to publish, or preparation of the manuscript.

## References

1. Hoft DF, Brown RM, Roodman ST. Bacille Calmette-Guerin vaccination enhances human gamma delta T cell responsiveness to mycobacteria suggestive of a memory-like phenotype. *J Immunol* 1998;161:1045-54.
2. Murphy AG, O'Keefe KM, Lalor SJ, et al. Staphylococcus aureus infection of mice expands a population of memory gammadelta T cells that are protective against subsequent infection. *J Immunol* 2014;192:3697-708.
3. Pitard V, Roumanes D, Lafarge X, et al. Long-term expansion of effector/memory Vdelta2-gammadelta T cells is a specific blood signature of CMV infection. *Blood* 2008;112:1317-24.
4. Ryan-Payseur B, Frencher J, Shen L, et al. Multieffector-functional immune responses of HMBPP-specific Vgamma2Vdelta2 T cells in nonhuman primates inoculated with *Listeria monocytogenes* DeltaactA prfA\*. *J Immunol* 2012;189:1285-93.
5. Shen Y, Zhou D, Qiu L, et al. Adaptive immune response of Vgamma2Vdelta2+ T cells during mycobacterial infections. *Science* 2002;295:2255-8.
6. Sheridan BS, Romagnoli PA, Pham QM, et al. gammadelta T cells exhibit multifunctional and protective memory in intestinal tissues. *Immunity* 2013;39:184-95.
7. Melandri D, Zlatareva I, Chaleil RAG, et al. The gammadeltaTCR combines innate immunity with adaptive immunity by utilizing spatially distinct regions for agonist selection and antigen responsiveness. *Nat Immunol* 2018;19:1352-1365.
8. Davey MS, Willcox CR, Hunter S, et al. The human Vdelta2(+) T-cell compartment comprises distinct innate-like Vgamma9(+) and adaptive Vgamma9(-) subsets. *Nat Commun* 2018;9:1760.
9. D'Ombra MC, Hansen DS, Simpson KM, et al. gammadelta-T cells expressing NK receptors predominate over NK cells and conventional T cells in the innate IFN-gamma response to *Plasmodium falciparum* malaria. *Eur J Immunol* 2007;37:1864-73.
10. D'Ombra MC, Robinson LJ, Stanisic DI, et al. Association of early interferon-gamma production with immunity to clinical malaria: a longitudinal study among Papua New Guinean children. *Clin Infect Dis* 2008;47:1380-7.
11. Hernandez-Castaneda MA, Happ K, Cattalani F, et al. gammadelta T Cells Kill *Plasmodium falciparum* in a Granzyme- and Granulysin-Dependent Mechanism during the Late Blood Stage. *J Immunol* 2020;204:1798-1809.
12. Jagannathan P, Kim CC, Greenhouse B, et al. Loss and dysfunction of Vdelta2(+) gammadelta T cells are associated with clinical tolerance to malaria. *Sci Transl Med* 2014;6:251ra117.
13. Jagannathan P, Lutwama F, Boyle MJ, et al. Vdelta2+ T cell response to malaria correlates with protection from infection but is attenuated with repeated exposure. *Sci Rep* 2017;7:11487.
14. Schofield L, Ioannidis LJ, Karl S, et al. Synergistic effect of IL-12 and IL-18 induces TIM3 regulation of gammadelta T cell function and decreases the risk of clinical malaria in children living in Papua New Guinea. *BMC Med* 2017;15:114.

15. Stanistic DI, Cutts J, Eriksson E, et al. gammadelta T cells and CD14+ monocytes are predominant cellular sources of cytokines and chemokines associated with severe malaria. *J Infect Dis* 2014;210:295-305.
16. Teirlinck AC, McCall MB, Roestenberg M, et al. Longevity and composition of cellular immune responses following experimental *Plasmodium falciparum* malaria infection in humans. *PLoS Pathog* 2011;7:e1002389.
17. Kobayashi F, Niikura M, Waki S, et al. *Plasmodium berghei* XAT: contribution of gammadelta T cells to host defense against infection with blood-stage nonlethal malaria parasite. *Exp Parasitol* 2007;117:368-75.
18. Kopacz J, Kumar N. Murine gamma delta T lymphocytes elicited during *Plasmodium yoelii* infection respond to *Plasmodium* heat shock proteins. *Infect Immun* 1999;67:57-63.
19. Mamedov MR, Scholzen A, Nair RV, et al. A Macrophage Colony-Stimulating-Factor-Producing gammadelta T Cell Subset Prevents Malarial Parasitemic Recurrence. *Immunity* 2018;48:350-363 e7.
20. Seixas E, Fonseca L, Langhorne J. The influence of gammadelta T cells on the CD4+ T cell and antibody response during a primary *Plasmodium chabaudi chabaudi* infection in mice. *Parasite Immunol* 2002;24:131-40.
21. Seixas EM, Langhorne J. gammadelta T cells contribute to control of chronic parasitemia in *Plasmodium chabaudi* infections in mice. *J Immunol* 1999;162:2837-41.
22. van der Heyde HC, Elloso MM, Chang WL, et al. Gamma delta T cells function in cell-mediated immunity to acute blood-stage *Plasmodium chabaudi adami* malaria. *J Immunol* 1995;154:3985-90.
23. Zaidi I, Duffy PE. Response to Comment on "gammadelta T Cells Are Required for the Induction of Sterile Immunity during Irradiated Sporozoite Vaccinations". *J Immunol* 2018;200:1533-1534.
24. Langhorne J, Mombaerts P, Tonegawa S. alpha beta and gamma delta T cells in the immune response to the erythrocytic stages of malaria in mice. *Int Immunol* 1995;7:1005-11.
25. Weidanz WP, Kemp JR, Batchelder JM, et al. Plasticity of immune responses suppressing parasitemia during acute *Plasmodium chabaudi* malaria. *J Immunol* 1999;162:7383-8.
26. Weidanz WP, LaFleur G, Brown A, et al. Gammadelta T cells but not NK cells are essential for cell-mediated immunity against *Plasmodium chabaudi* malaria. *Infect Immun* 2010;78:4331-40.
27. Medeiros MM, da Silva HB, Reis AS, et al. Liver accumulation of *Plasmodium chabaudi*-infected red blood cells and modulation of regulatory T cell and dendritic cell responses. *PLoS One* 2013;8:e81409.
28. van der Heyde HC, Batchelder JM, Sandor M, et al. Splenic gammadelta T cells regulated by CD4+ T cells are required to control chronic *Plasmodium chabaudi* malaria in the B-cell-deficient mouse. *Infect Immun* 2006;74:2717-25.
29. Sun JC, Beilke JN, Lanier LL. Adaptive immune features of natural killer cells. *Nature* 2009;457:557-61.
30. Sun JC, Beilke JN, Lanier LL. Immune memory redefined: characterizing the longevity of natural killer cells. *Immunol Rev* 2010;236:83-94.
31. Schroeder JT, Chichester KL, Bieneman AP. Toll-like receptor 9 suppression in plasmacytoid dendritic cells after IgE-dependent

- activation is mediated by autocrine TNF-alpha. *J Allergy Clin Immunol* 2008;121:486-91.
32. Russ BE, Olshanksy M, Smallwood HS, et al. Distinct epigenetic signatures delineate transcriptional programs during virus-specific CD8(+) T cell differentiation. *Immunity* 2014;41:853-65.
  33. Misiak A, Wilk MM, Raverdeau M, et al. IL-17-Producing Innate and Pathogen-Specific Tissue Resident Memory gammadelta T Cells Expand in the Lungs of Bordetella pertussis-Infected Mice. *J Immunol* 2017;198:363-374.
  34. Jensen KD, Su X, Shin S, et al. Thymic selection determines gammadelta T cell effector fate: antigen-naive cells make interleukin-17 and antigen-experienced cells make interferon gamma. *Immunity* 2008;29:90-100.
  35. Kreslavsky T, Savage AK, Hobbs R, et al. TCR-inducible PLZF transcription factor required for innate phenotype of a subset of gammadelta T cells with restricted TCR diversity. *Proc Natl Acad Sci U S A* 2009;106:12453-8.
  36. Ribot JC, deBarros A, Pang DJ, et al. CD27 is a thymic determinant of the balance between interferon-gamma- and interleukin 17-producing gammadelta T cell subsets. *Nat Immunol* 2009;10:427-36.
  37. Melichar HJ, Narayan K, Der SD, et al. Regulation of gammadelta versus alphabeta T lymphocyte differentiation by the transcription factor SOX13. *Science* 2007;315:230-3.
  38. Malhotra N, Narayan K, Cho OH, et al. A network of high-mobility group box transcription factors programs innate interleukin-17 production. *Immunity* 2013;38:681-93.
  39. Uematsu S, Jang MH, Chevrier N, et al. Detection of pathogenic intestinal bacteria by Toll-like receptor 5 on intestinal CD11c+ lamina propria cells. *Nat Immunol* 2006;7:868-74.
  40. Hamada S, Umemura M, Shiono T, et al. IL-17A produced by gammadelta T cells plays a critical role in innate immunity against listeria monocytogenes infection in the liver. *J Immunol* 2008;181:3456-63.
  41. Shibata K, Yamada H, Hara H, et al. Resident Vdelta1+ gammadelta T cells control early infiltration of neutrophils after Escherichia coli infection via IL-17 production. *J Immunol* 2007;178:4466-72.
  42. Simonian PL, Roark CL, Diaz del Valle F, et al. Regulatory role of gammadelta T cells in the recruitment of CD4+ and CD8+ T cells to lung and subsequent pulmonary fibrosis. *J Immunol* 2006;177:4436-43.
  43. Brandes M, Willimann K, Moser B. Professional antigen-presentation function by human gammadelta T Cells. *Science* 2005;309:264-8.
  44. Howard J, Loizon S, Tyler CJ, et al. The Antigen-Presenting Potential of Vgamma9Vdelta2 T Cells During Plasmodium falciparum Blood-Stage Infection. *J Infect Dis* 2017;215:1569-1579.
  45. Tyler CJ, McCarthy NE, Lindsay JO, et al. Antigen-Presenting Human gammadelta T Cells Promote Intestinal CD4(+) T Cell Expression of IL-22 and Mucosal Release of Calprotectin. *J Immunol* 2017;198:3417-3425.
  46. Tan AC, Eriksson EM, Kedzierska K, et al. Polyfunctional CD8(+) T cells are associated with the vaccination-induced control of a novel recombinant influenza virus expressing an HCV epitope. *Antiviral Res* 2012;94:168-78.
  47. Brugat T, Cunningham D, Sodenkamp J, et al. Sequestration and histopathology in Plasmodium chabaudi malaria are influenced by the

- immune response in an organ-specific manner. *Cell Microbiol* 2014;16:687-700.
48. O'Donovan SM, Dalton JP. An improved medium for *Plasmodium chabaudi* in vitro erythrocyte invasion assays. *J Eukaryot Microbiol* 1993;40:152-4.
  49. Liao Y, Smyth GK, Shi W. The Subread aligner: fast, accurate and scalable read mapping by seed-and-vote. *Nucleic Acids Res* 2013;41:e108.
  50. Liao Y, Smyth GK, Shi W. featureCounts: an efficient general purpose program for assigning sequence reads to genomic features. *Bioinformatics* 2014;30:923-30.
  51. Robinson MD, McCarthy DJ, Smyth GK. edgeR: a Bioconductor package for differential expression analysis of digital gene expression data. *Bioinformatics* 2010;26:139-40.
  52. Ritchie ME, Phipson B, Wu D, et al. limma powers differential expression analyses for RNA-sequencing and microarray studies. *Nucleic Acids Res* 2015;43:e47.
  53. Robinson MD, Oshlack A. A scaling normalization method for differential expression analysis of RNA-seq data. *Genome Biol* 2010;11:R25.
  54. Law CW, Chen Y, Shi W, et al. voom: Precision weights unlock linear model analysis tools for RNA-seq read counts. *Genome Biol* 2014;15:R29.
  55. McCarthy DJ, Smyth GK. Testing significance relative to a fold-change threshold is a TREAT. *Bioinformatics* 2009;25:765-71.
  56. Phipson B, Lee S, Majewski IJ, et al. Robust Hyperparameter Estimation Protects against Hypervariable Genes and Improves Power to Detect Differential Expression. *Ann Appl Stat* 2016;10:946-963.
  57. Benjamini YaH, Y. Controlling the False Discovery Rate: A Practical and Powerful Approach to Multiple Testing. *Journal of the Royal Statistical Society: Series B (Methodological)* 1995;57:289-300.
  58. Wu D, Lim E, Vaillant F, et al. ROAST: rotation gene set tests for complex microarray experiments. *Bioinformatics* 2010;26:2176-82.

## Figure 1

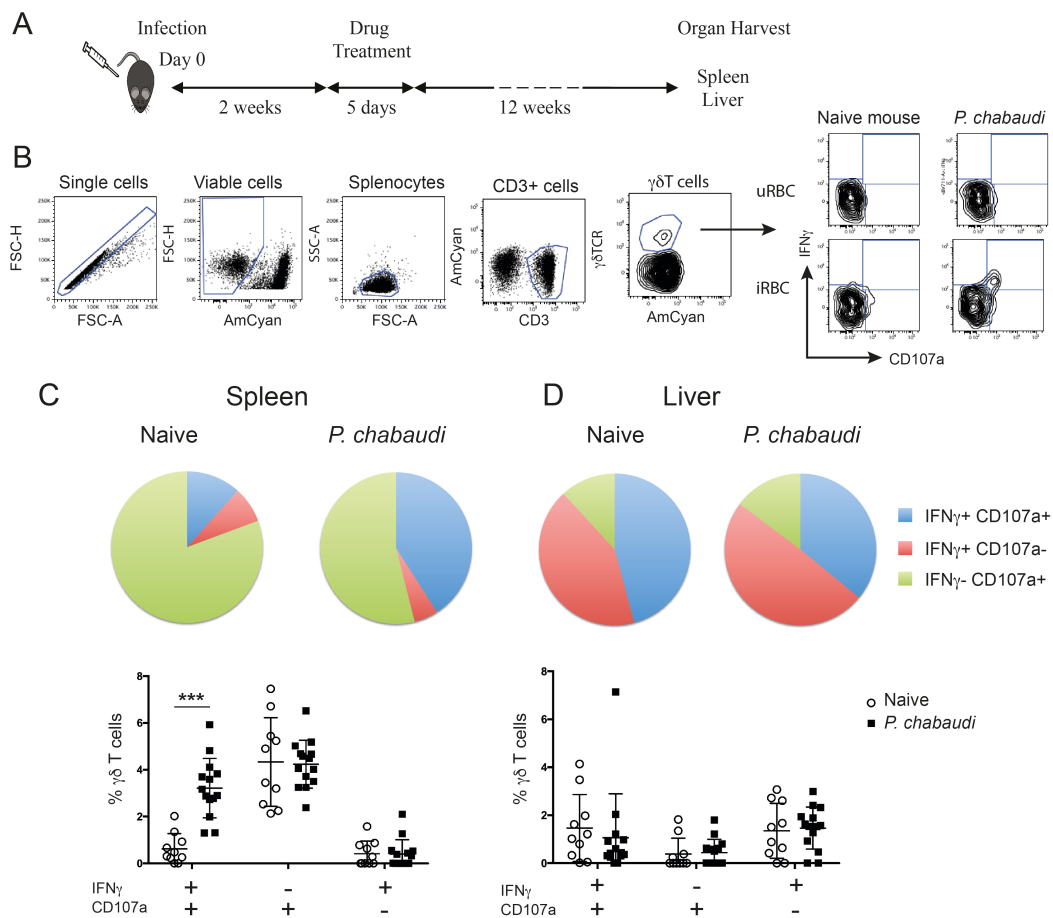


**Figure 1. Increased frequency of IFN $\gamma$ <sup>+</sup>CD107a<sup>+</sup> $\gamma\delta$  T cells in previously infected mice.** A) C57BL/6 mice were infected with *P. chabaudi* and then drug-treated with chloroquine and pyrimethamine two weeks later. Twelve weeks following completion of drug-treatment cells were isolated and stimulated with iRBCs or uRBCs and frequencies of IFN $\gamma$ <sup>+</sup> and/or CD107a<sup>+</sup> C) splenocytes and D) liver lymphocytes from previously infected mice (*P. chabaudi* black squares, n=14) and naïve control (white circles, n=10) after stimulation. In the pie chart the data are presented as the frequency of IFN $\gamma$ <sup>+</sup> CD107a<sup>+</sup> (blue), IFN $\gamma$ <sup>+</sup> CD107a<sup>-</sup> (red) and IFN $\gamma$ <sup>-</sup> CD107a<sup>+</sup> (green)  $\gamma\delta$  T cells in each group following uRBC background subtraction. The data in the scatter plot are presented as mean  $\pm$  SD following uRBC background subtraction. The data represent two independent experiments. Statistical analysis was performed using Student's t-tests. \*\*\*P < 0.001

## Figure 2

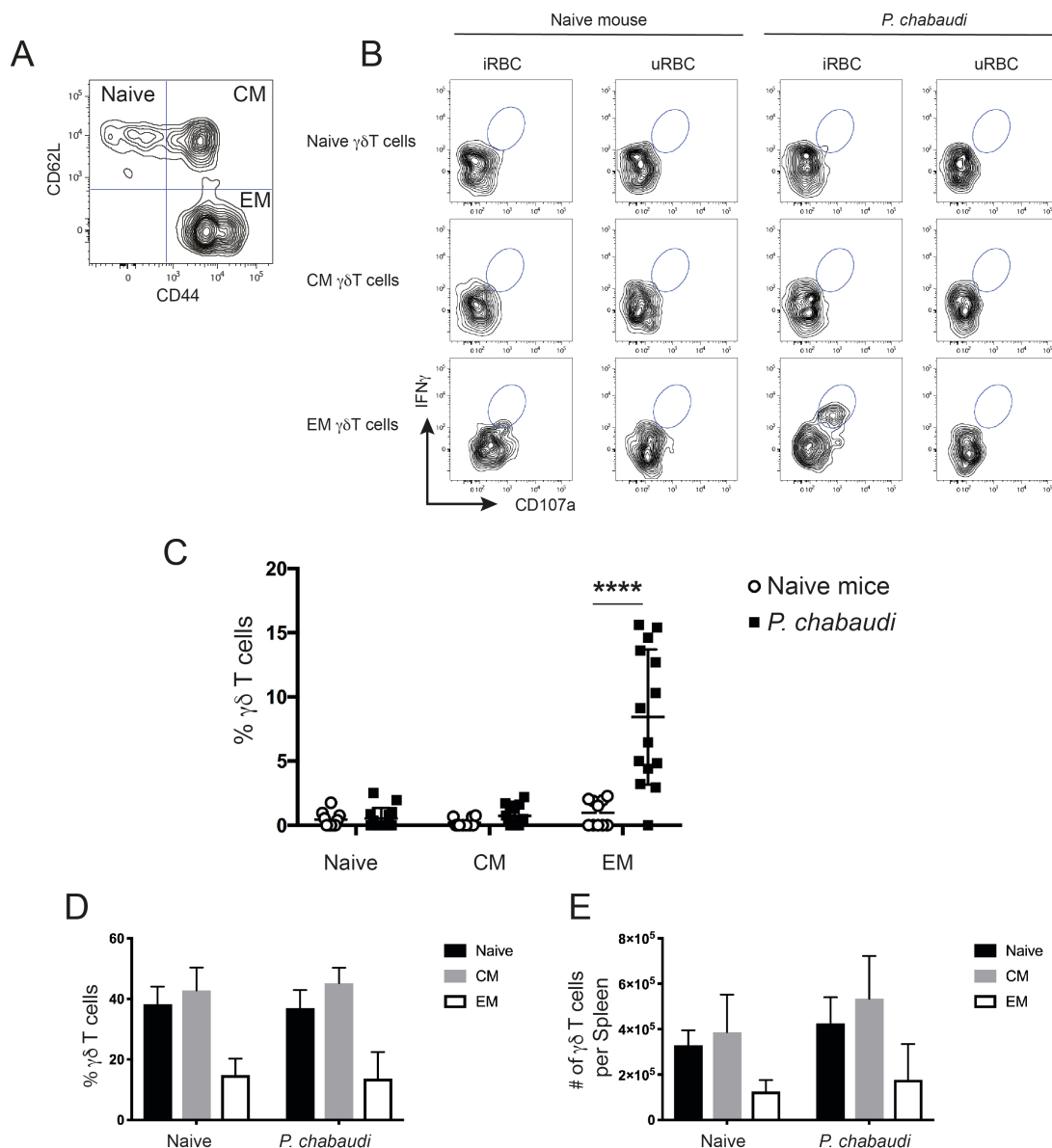


**Figure 2. *In vitro* re-stimulated and activated  $\gamma\delta$  T cells express CD44, but lack CD62L expression.** Splenocytes from previously infected and drug treated mice and naïve controls were restimulated *in vitro* with iRBC or uRBCs. Representative contour plot to A) distinguish between CD62L<sup>+</sup>CD44<sup>-</sup> (Naïve), CD62L<sup>+</sup>CD44<sup>+</sup> (CM) and CD62L<sup>-</sup>CD44<sup>+</sup> EM  $\gamma\delta$  T cells. B) Representative contour plots showing frequency of IFN $\gamma$ <sup>+</sup>CD107a<sup>+</sup>  $\gamma\delta$  T cells for each subset after 24 h stimulation with either iRBC or uRBC from naïve or *P. chabaudi* pre-exposed mice. C) Summary of IFN $\gamma$ <sup>+</sup>CD107a<sup>+</sup> naïve, CM and EM  $\gamma\delta$  T cells after iRBC stimulation following subtraction of background levels determined from uRBC stimulations in previously *P. chabaudi*-infected mice (filled squares; n=14) and naïve controls (open circles; n=10). Overall D) frequency and E) number of  $\gamma\delta$  T cells per spleen of naïve, CM and EM  $\gamma\delta$  T cells (mean $\pm$ SD) in naïve or *P. chabaudi* pre-exposed mice. The data represent two independent experiments. Statistical analysis was performed using C-E) Student's t-tests \*\*\*\*P < 0.0001



## Figure 3

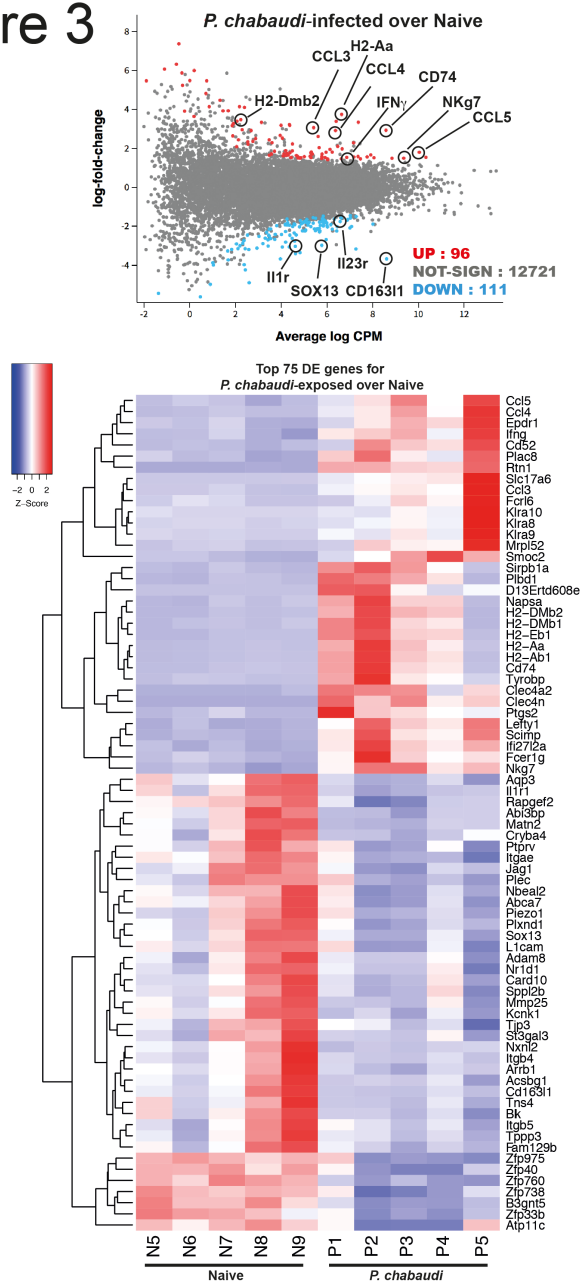


**Figure 3. RNA-sequencing of EM  $\gamma\delta$  T cells from *P. chabaudi* pre-exposed mice and naïve controls.** EM  $\gamma\delta$  T cells from drug-treated naïve mice (n=5 donors) and *P. chabaudi* pre-exposed mice (n=5) were FACS sorted followed by RNA extraction and RNA-sequencing. Differential gene expression for *P. chabaudi* over naïve mice was summarized in A) mean-difference (MD) plot of log<sub>2</sub> expression fold-changes against the average log-expressions for each gene. The differentially expressed (DE) genes relative to a fold change threshold of 1.5 are highlighted, with points colored in red and blue indicating up- and down regulated genes respectively. B) Heatmap of the expressions of the top 75 DE genes between *P. chabaudi* and naïve mice. Each vertical column represents genes for each mouse. For a given gene the red and blue coloring indicates increased and decreased expression in *P. chabaudi* compared to naïve respectively.

## Figure 4

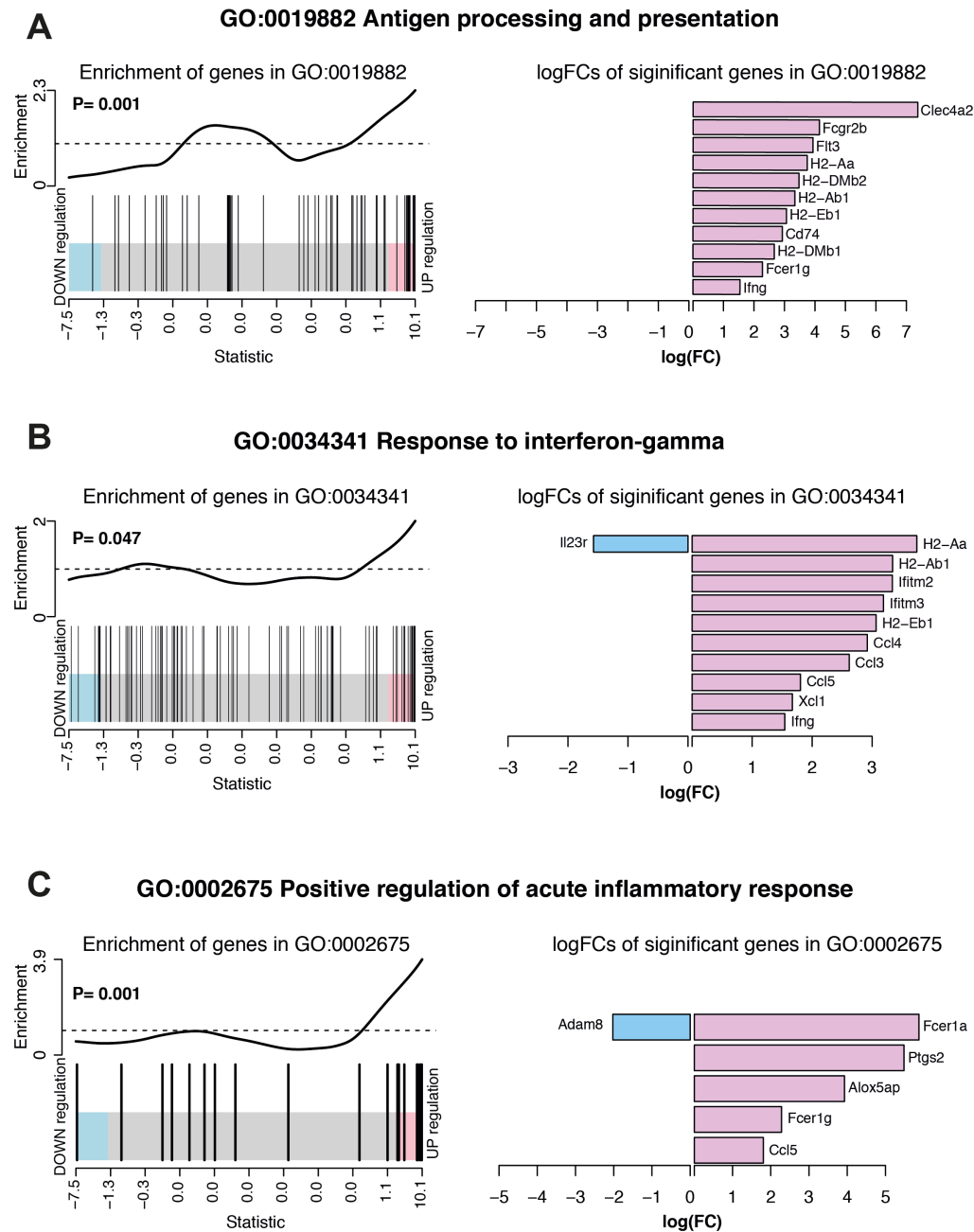
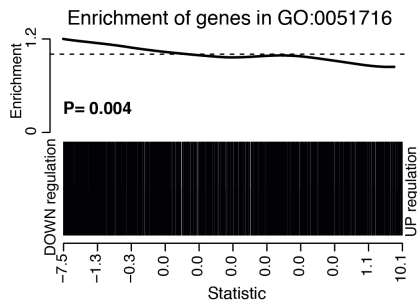


**Figure 4. Summary of significant up or down regulated genes in selected upregulated biological processes.** Barcode plots for enrichment of the pathway genes along with p-values relative to gene enrichment tested using ROAST method (left panel) and bar graphs of log fold changes of the significant pathway genes (right panel) for pathways A) GO:0019882 antigen processing and presentation, B) GO:0034341 response to IFN $\gamma$  and C) GO:0002675 positive regulation of acute inflammatory response. The barcode plot ranks genes right to left from most up- to most down regulated in *P. chabaudi* mice, with genes in the pathways marked by vertical bars. The bar graph show log fold changes of significantly upregulated and down regulated genes in the pathway using pink bars and blue bars respectively.

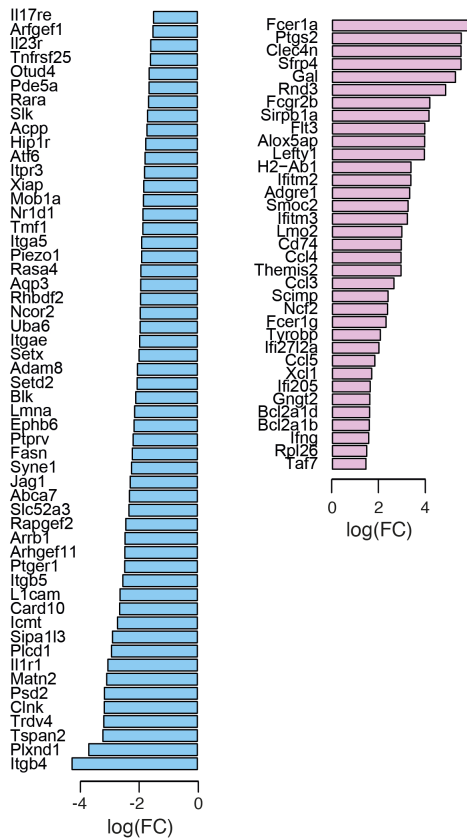
## Figure 5

A

GO:0051716 Cellular response to stimulus

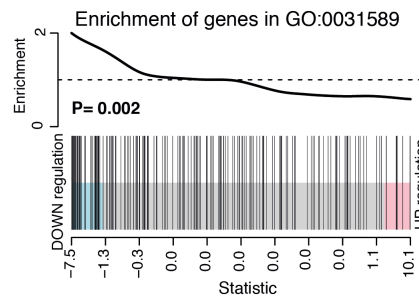


logFCs of significant genes in GO:0051716



B

GO:0031589 Cell-substrate adhesion



logFCs of significant genes in GO:0031589

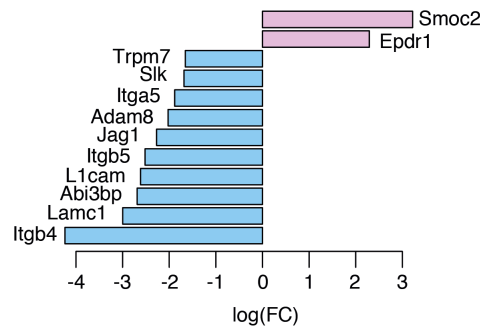


**Figure 5. Summary of significant up or down regulated genes in selected down regulated biological processes.** Barcode plots for enrichment of the pathway genes along with p values relative to gene enrichment tested using ROAST method (top panel) and bar graphs of log fold changes of the significant pathway genes (bottom panel) for pathways A) GO:0051716 cellular response to stimulus and B) GO:0031589 cell-substrate adhesion. The barcode plot ranks genes right to left from most up- to most down regulated in *P. chabaudi* mice, with genes in the pathways marked by vertical bars. The bar graph show log fold changes of significantly upregulated and down regulated genes in the pathway using pink bars and blue bars respectively.

Figure 6

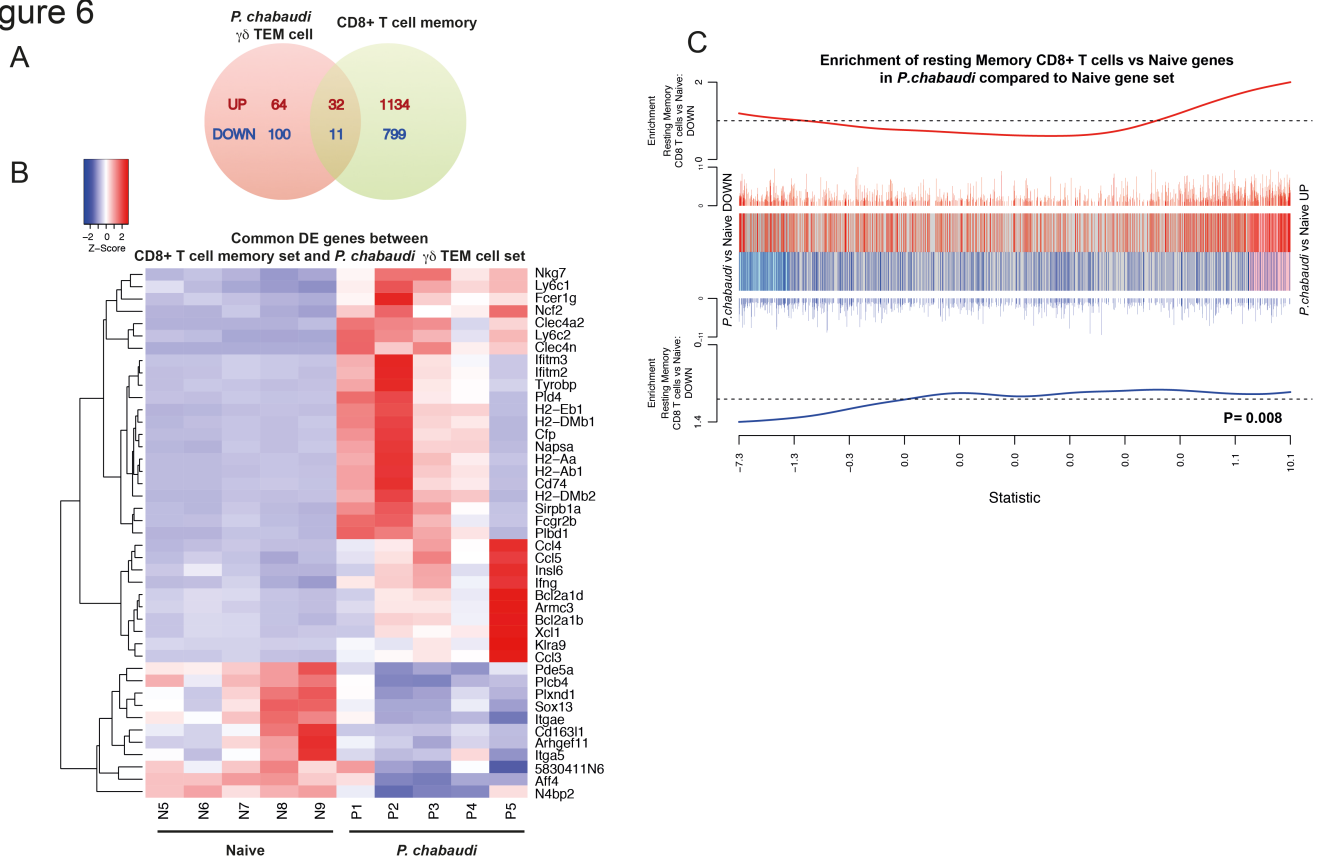


**Figure 6. Differentially expressed genes in *P. chabaudi* pre-exposed  $\gamma\delta$  T cells are positively correlated with differentially expressed genes in  $CD8^+$  memory T cells.** A) Venn diagram showing the number of overlapping and non-overlapping up-regulated (red) and down regulated (blue) genes. B) Heatmap of the gene expression relative to *P. chabaudi* pre-exposed  $\gamma\delta$  T cells data for the genes commonly significantly regulated (overlapping DE genes) between *P. chabaudi* pre-exposed  $\gamma\delta$  T cells data and  $CD8^+$  memory T cell data. Each vertical column represents genes for each mouse. For a given gene the red and blue coloring indicates increased and decreased expression in *P. chabaudi* compared to naïve respectively. C) Barcodeplot for the enrichment of DE genes in the resting  $CD8^+$  memory T cell data in *P. chabaudi* compared to naïve in the *P. chabaudi* pre-exposed  $\gamma\delta$  T cell data, along with the ROAST p-value for the gene set testing.